PAPER

Check for updates

Preparation and characterization of attapulgite-supported phase change energy storage materials

Weijun Hu,[a] Shaohui Lin, ID [a] Yufeng Cao,[b] Xianshe Feng[c] and Qinmin Pan ID *[a]

Phase change materials (PCMs) for the charge and discharge of thermal energy at a nearly constant temperature are of interest for thermal energy storage and management, and porous materials are usually used to support PCMs for preventing the liquid leakage and shape instability during the phase change process. Compared with commonly used polymer matrices and porous carbons, mineral materials with naturally occurring porous structures have obvious advantages such as cost-saving and abundant resources. Attapulgite (ATP) is a clay mineral with natural porous structures, which can be used to contain PCMs for thermal energy storage. However, the poor compatibility between ATP and PCMs is a significant defect that has rarely been studied. Herein, a facile one-step organic modification method of ATP was developed and the chlorosilane-modified ATP (Si-ATP) possesses great hydrophobic and lipophilic properties. Three types of ATP with different compatibility and pore volumes were used as the supports and paraffin as the energy storage units to fabricate a series of form-stable PCMs (FSPCMs). The results showed that the shape-stabilized ability of Si-ATP for paraffin was significantly enhanced, and the Si-ATP supported FSPCM yielded an optimal latent heat of 83.7 J g^{-1}, which was 64.4% higher than that of the pristine ATP based composite. Meanwhile, the thermal energy storage densities of the resulting FSPCMs were gradually increased with an increase in the pore volumes of the three supporting materials. These results may provide a strategy for preparing porous materials as containers to realize the shape stabilization of PCMs and improve the thermal energy storage densities of the resulting FSPCMs.

1. Introduction

Phase change materials (PCMs) are attracting attention for thermal energy storage based on charging and discharging of latent heat *via* a reversible phase transition, and have the potential to alleviate energy shortage and environmental concerns,[1–6] and their applications in storing solar energy and harnessing waste heat are especially of interest. The thermo-regulation functionality of PCMs has been used for thermal management in lithium-ion batteries,[7] residential insulation walls,[8] thermo-regulating textiles,[9] deployable panels in electronic devices[10] and refrigerators,[11] *etc.*

Generally, PCMs can be divided into three types based on their states of phase transitions: solid–gas PCMs (SGPCMs), solid–liquid PCMs (SLPCMs), and solid–solid PCMs (SSPCMs).[12–14] Among them, SLPCMs have been studied

extensively because of their high latent heat storage capacity, little or no super-cooling, minimal volume change, and favorable phase change temperature range,[15,16] these common SLPCMs include alkanes, fatty acids and polyethylene glycols. However, the inherent drawbacks of SLPCMs are the liquid leakage and shape instability during the phase change process, leading to device smudging and decreased heat storage capacity. One of effective strategies to overcome above critical issues is by incorporating appropriate porous materials into the PCMs for fabricating form-stable PCMs (FSPCMs),[17] and these porous materials include polymer matrices,[18,19] mineral materials such as vermiculite[20] and porous carbon materials.[21] The synthesis of polymer matrices and porous carbons is usually complicated and costly, on the contrary, mineral materials with naturally occurring porous structures have inherent advantages as scaffolds for the shape stabilization of PCMs, including abundance in nature, good mechanical and thermal stability, cost-saving, *etc.*

Attapulgite(ATP) is a hydrous magnesium aluminum silicate clay mineral with layer-chain structures, which consists of a double chain of Si–O tetrahedra running parallel to the long axis, and at the upper and lower parts of each double chain are linked by a layer of octahedral magnesium atoms in 6-fold coordination. The chains form a network of strips that are

[a]*Green Polymer Engineering & Catalysis Technology Laboratory, College of Chemistry, Chemical Engineering and Material Science, Soochow University, 199 Ren-ai Road, Suzhou 215123, Jiangsu Province, People's Republic of China. E-mail: qpan@suda.edu.cn*

[b]*School of Chemistry and Chemical Engineering, Nantong University, 9 Se-yuan Road, Nantong 226019, China*

[c]*Department of Chemical Engineering, University of Waterloo, 200 University Ave. West, Waterloo, ON, N2L 3G1, Canada*

joined together only along the edges, thus, the overall structure of ATP resembles like a channeled wall where every second brick is missing. The special structure of ATP make it possessing many excellent properties, such as large specific surface area and porous structure, good mechanical and thermal stability, non-toxicity, good rheology, etc.[22–24] Because the porous structure of ATP can provide a capillary force and adsorption capacity to achieve the shape stabilization of PCMs, it has been used to contain PCMs for thermal energy storage and management.[25–28] For instance, Li et al.[25] attempted to use ATP as the supporting material for capric-palmitic binary fatty acid (CA-PA) to prepare FSPCMs by a vacuum assisted method, and the optimal adsorption mass of ATP to the CA-PA reached about 35.0 wt%, yielding a thermal energy storage density of 48.2 J g^{-1}. Shi et al.[27] used the ATP as the scaffold of paraffin for thermal energy storage, and the composite yielded a latent heat of fusion for 59.3 J g^{-1}. The study showed that the trombe walls containing ATP/paraffin could effectively reduce the fluctuation of indoor ambient temperature and improve the comfortability of residence. Liang et al.[28] synthesized a spongy attapulgite (S-ATP) with three-dimensional porous structures through a polymerization method. The S-ATP had increased pore size and good compatibility with PCMs, as a result, the S-ATP's supporting capacity for n-carboxylic acid (36.6–37.7 wt%) was much higher than the ATP (20.9–27.0 wt%) and the thermal energy storage densities of the resulting composites increased to 72.6–82.4 J g^{-1}, but the preparation process of n-carboxylic acid/S-ATP was relatively complicated and expensive. However, the Liang's work illustrated that the poor compatibility between the ATP and PCMs is a significant defect restricting its supporting capacity for PCMs, which may result in lower thermal energy storage capacity as compared to polymer matrices and porous carbons.

In this work, we offered a facile one-step organic modification method to solve the poor compatibility problem of the ATP with organic PCMs. Three types of ATP with different compatibility and pore volumes were used as the supporting materials and paraffin as the energy storage units to fabricate a series of FSPCMs. The properties of the supporting materials and FSPCMs were evaluated and characterized using physisorption analyzer, scanning electron microscopy (SEM), transmission electron microscope (TEM), thermo-gravimetric analysis (TGA), X-ray diffraction (XRD), differential scanning calorimetry, etc.

2. Experimental

2.1 Materials

Ethanol, hydrochloric acid, sodium hydroxide, acetone and pyridine were all analytical grade and purchased from Jiangsu Argon Krypton Xenon Material Technology Co.,Ltd. Paraffin (T_m = 56–58 °C) was obtained from Sino Pharm Chemical Reagent Co.,Ltd. Trimethylchlorosilane (TMCS, ≥99.0%GC), triethylchlorosilane (TESC, ≥98wt%), n-octyltrichlorosilane (≥95 wt%) and dimethyl octadecyl chlorosilane (≥97 wt%) were purchased from Suzhou Gretel Pharmaceutical Technology Co.,Ltd, and were used as the modification reagents for ATP, the chemical structures of these modification reagents were shown in Fig. 1. All chemicals were used as received unless otherwise noted. Deionized water was used throughout the studies. Attapulgite [$Mg_5Si_8O_{20}(OH)_2(OH_2)_4 \cdot 4H_2O$] was obtained from Jiuchuan Clay Technology Co.,Ltd, Jiangsu Province, China.

2.2 Organic modification process of ATP

The ATP was activated by 3.0 mol L^{-1} of hydrochloric acid for 6–8 h and denoted as A-ATP. Then, 1.0 g of A-ATP was added into a beaker filled with 30.0 ml of acetone and treated with ultrasound for 10 min, followed by the addition of 0.5 ml of NaOH (1.0 M) and 4.0 ml of TMCS. The solution was stirred at room temperature for 18–24 h. During the course of reaction, a trace of pyridine was added to neutralize hydrochloric acid produced by the condensation reaction between the chloride group of chlorosilane reagents and hydroxyl groups of A-ATP. After completing the reaction, the product was filtered and successively rinsed with distilled water and anhydrous alcohol about 3–5 times. The purified product was dried at 80 °C in an drying oven until a final white powder was obtained and marked as Si-ATP. Additional Si-ATPs were also prepared in the same manner using TESC (2.0 ml), n-octyltrichlorosilane (2.0 ml) and dimethyl octadecyl chlorosilane (41.1 mg) as the chlorosilane modification reagents.

2.3 Preparation of FSPCMs

2.3.1 Solution absorption method. 5.0 g of paraffin was melted at 80 °C in a 50 ml conical beaker, and then 30.0 ml of ethanol was added to form a homogeneous solution.
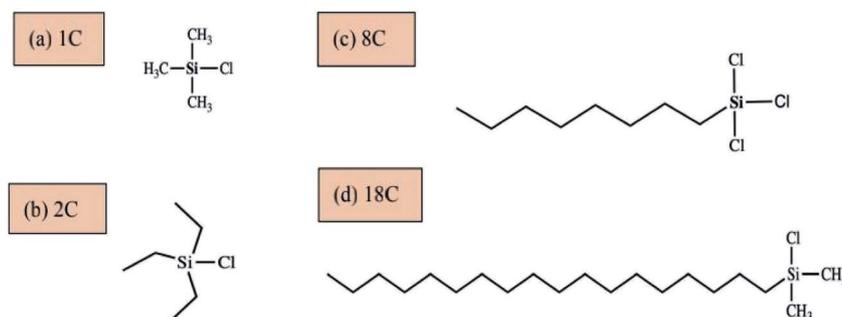

Fig. 1 Chemical structures of these chlorosilane modification reagents: (a) trimethylchlorosilane (1C); (b)triethylchlorosilane (2C); (c) n-octyltrichlorosilane (8C); (d) dimethyl octadecyl chlorosilane (18C).

Afterwards, 1.0 g of Si-ATP was added into the above solution, and the mixture was stirred for 5 h to reach absorption equilibrium. Then, the mixture was thermally filtered and dried at 80–100 °C in an drying oven until the weight of composite was constant and no liquid leakage was detected. For comparison, the FSPCMs with ATP and A-ATP as the supporting materials were prepared in the same manner, and the three FSPCMs were denoted as ATP/paraffin, A-ATP/paraffin and Si-ATP/paraffin, respectively.

2.3.2 Vacuum impregnation method. Si-ATP and paraffin in predetermined amounts were transferred into a triangular flask and heated to 85 °C under a vacuum condition, which allowed the melting paraffin to penetrate into the pore canals of Si-ATP. The final FSPCM was obtained until the mass of composite reached constant and no liquid leakage was detected. The composites based on ATP and A-ATP as the supporting matrices were also obtained in the same manner, and the three FSPCMs were denoted as V-ATP/paraffin, V-A-ATP/paraffin and V-Si-ATP/paraffin, respectively, to distinguish from the composites prepared *via* solution absorption method.

2.4 Characterizations

The chemical structures of these Si-ATPs were investigated by a Fourier transformation infrared spectroscope (FT-IR, Vertex 70 and Hyperion 2000, wavenumber range: 600–4000 cm^{-1}). Pore structures of the supporting materials were characterized *via* a physisorption analyzer (ASAP2020M, Micromeritics). The surface contact angles of these Si-ATPs were measured with a DataphysicsOCA20 contact angle instrument (Stuttgart, Germany). The crystalline properties of paraffin in the composites were investigated using an X-ray diffractometer (Bruker D8-advance with Cu $K\alpha$ radiation wavelength $k = 0.15418$ nm). Morphologies of the supporting materials and FSPCMs were observed under a scanning electron microscope (SEM, Gemini SEM 300) and field emission transmission electron microscope (TEM, Tecnai G2F20). The thermal energy storage properties of pure paraffin and FSPCMs were determined using a differential scanning calorimeter (DSC Q2500, TA Instruments Inc.) at a heating and cooling rate of 10 °C min^{-1} (each simple was about 5.0 mg, temperature range from 0–100 °C) in a nitrogen atmosphere. The thermal gravimetric analysis (TGA, TA-Q4000 series instruments) of the samples was conducted to evaluate their thermal stability. In addition, the samples were subjected to thermal durability tests with DSC after 200 cycles of repeated melting and cooling process.

3. Results and discussion

3.1 Chemical properties of Si-ATPs

Fig. 2(a) shows the FT-IR spectra of Si-ATPs. It was revealed that the ATP exhibits absorption bands of hydroxyl groups at 3554 and 1653 cm^{-1}, which are ascribed to the –OH stretching and –OH bending vibrations, respectively. The characteristic band at 1026 cm^{-1} is attributed to Si–OH of ATP, and the absorption bands at 984 and 796 cm^{-1} are ascribed to the Si–O–Si stretching vibrations of ATP.[29,30] The characteristic absorption bands of A-ATP are consistent with those of ATP, indicating that a moderate acid-activation treatment did not affect the chemical structures of ATP. The characteristic absorption bands of ATP are also shown in the FT-IR spectra of Si-ATPs, in addition to the new absorption bands at 2848 and 2923 cm^{-1} derived from the asymmetrical stretching vibrations and symmetrical stretching vibrations of –CH$_2$–, respectively. It is worth mentioning that the absorption peaks of Si-ATP(1C) at 2848 and 2923 cm^{-1} were very weak as compared to other Si-ATPs, presumably due to the shortest alkyl chain of TMCS among the four chlorosilane modification reagents. The dispersibility in toluene of Si-ATPs was investigated, and the results as shown in Fig. 2(b). When the same quantity of Si-ATPs was each added to 10.0 ml of toluene, upon ultrasonic treatment for 5 min, all Si-ATPs were well dispersed in toluene without settling down immediately as compared to unmodified counterparts, but they all precipitated completely after 10 min. The dispersibility result of Si-ATPs is different from what was observed by Yang's work[31] that grafting longer lengths of alkyl chain onto graphene could form a more stable suspension solution in organic solvents.

The liquid paraffin absorption test was carried out by Si-ATPs, the results as illustrated in Fig. 3(a). Compared with ATP and A-ATP, the Si-ATPs could well absorb the liquid paraffin
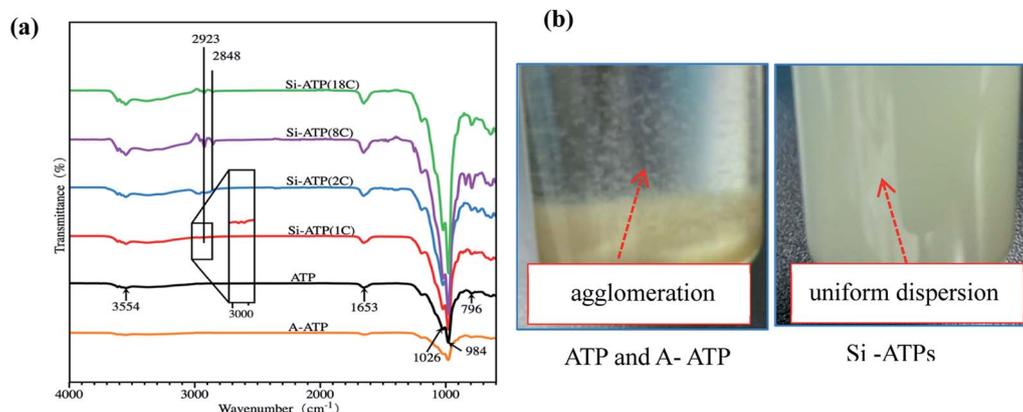

Fig. 2 FT-IR spectra and dispersibility in toluene of these Si-ATPs: (a) FT-IR spectra results; (b) pictures of Si-ATPs dispersed in toluene.
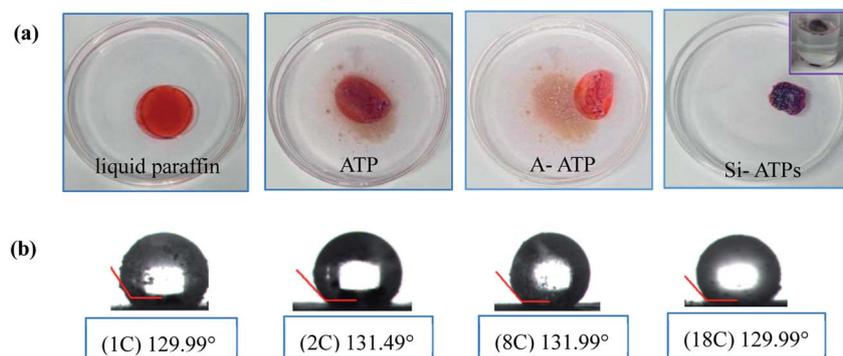
Fig. 3 (a) Observation of ATP, A-ATP and Si-ATPs absorbed the liquid paraffin (dyed with red oil for easy observation) in water; (b) the interfacial hydrophobic contact angles of Si-ATPs.

and still float on the surface of the water after absorption. Furthermore, as shown in Fig. 3(b), the interfacial hydrophobic contact angles of Si-ATPs were all about $131.0 \pm 1.0°$, demonstrating that Si-ATPs have great hydrophobic and lipophilic properties.

Overall, the above results demonstrated that the organic modification method in this study is applicable for ATP, which is environmental-friendly and cost-effective to make ATP has great lipophilic property for enhancing its compatibility with organic PCMs. In the following experiment, Si-ATP(1C) was selected as a supporting material to prepare FSPCMs. Unless otherwise mentioned, Si-ATP(1C) was briefed denoted as Si-ATP in the following description.

3.2 Morphologies and pore structures of the supporting materials

Morphologies of the three porous materials (ATP, A-ATP and Si-ATP) used as the supports for fabricating FSPCMs were investigated with SEM and TEM, and the results were shown in Fig. 4. Fig. 4(a and d) and (b and e) shows that ATP was present at an aggregated state which is detrimental to forming FSPCMs, while the A-ATP became more dispersed, because a moderate acid-
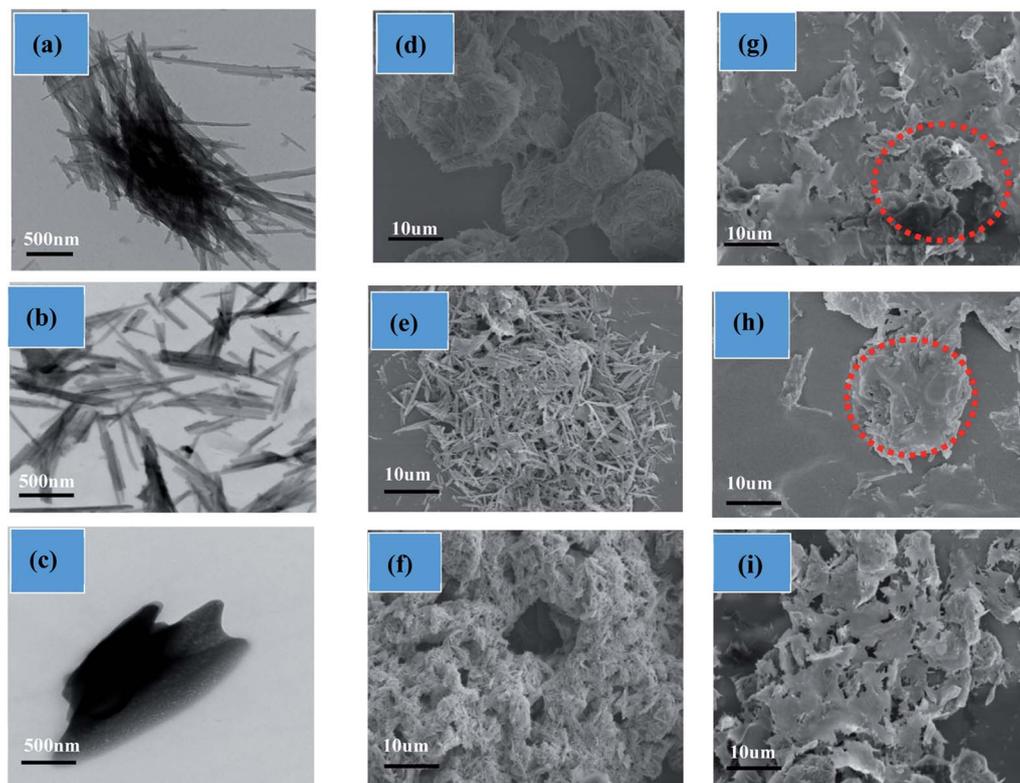

Fig. 4 TEM images of ATP (a), A-ATP (b) and Si-ATP(c); SEM images of ATP (d), A-ATP(e), Si-ATP(f), ATP/paraffin (g), A-ATP/paraffin (h) and Si-ATP/paraffin (i).

activation could reduce the surface energy and cause disaggregation between the fiber bundles of ATP.[22,24] The Si-ATP displays honeycomb porous structures with a fluffy state (Fig. 4(c)). In addition, the TEM image of Si-ATP shows a structure with a smooth surface and granular dispersion(Fig. 4(f)), resulting from the TMCS modification of the ATP's surface.

The pore structures of the three porous materials were evaluated with nitrogen adsorption at 77 K, and the results are presented in Table 1 and Fig. 5. As shown in Fig. 5(a), all samples exhibited type IV adsorption and desorption isotherms accompanied with small H_3 hysteresis loops, which showed mesoporous structures according to the IUPAC classification.[32,33] The total pore volumes estimated from the amount of gas adsorbed at $P/P_0 = 0.99$ were 0.38, 0.42 and 0.46 ml g^{-1} with
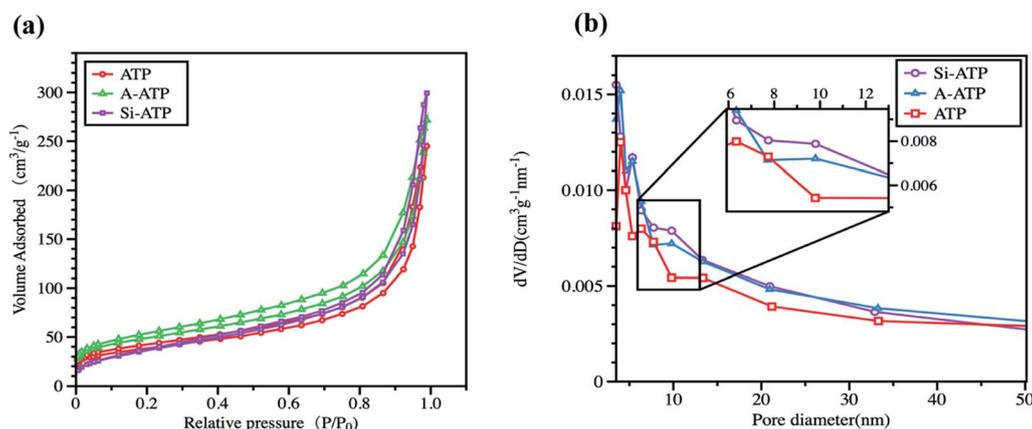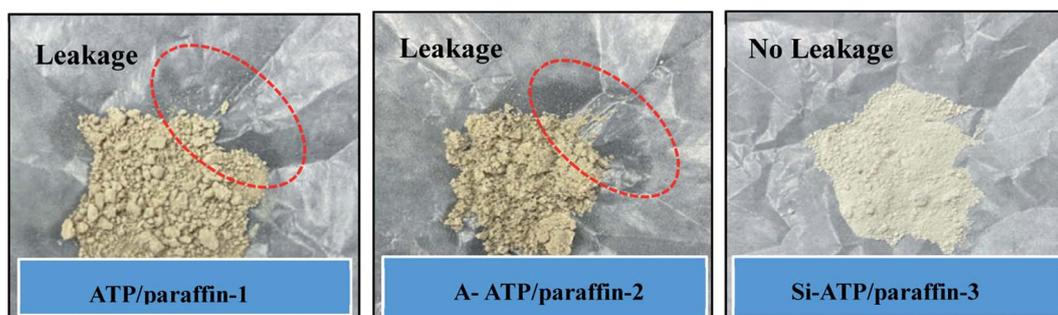
a slight increase for ATP, A-ATP and Si-ATP, respectively. The cavities of ATP were increased due to a moderate acid-activation could leach of some metal ions from its partial tetrahedral and octahedral sites,[22,24,34] and the TMCS-modified ATP become more fluffy for the presence of alkyl group, which made the pore volumes of Si-ATP was further increased as compared to A-ATP. The Barrett–Joyner–Halenda (BJH) pore size distributions of the three porous materials were depicted in Fig. 5(b), all samples were shown to be mesoporous (pore size 2–50 nm), and the Si-ATP had more mesopores in the pore size range of 6–13 nm, which also accounts for the pore volumes of Si-ATP were slightly higher than those of ATP and A-ATP. Furthermore, the average pore diameters of ATP, A-ATP and Si-ATP were approximately 11.2, 9.7 and 13.6 nm, respectively. As some literature reported that supporting materials with mesoporous structures are beneficial to support PCMs due to their proper capillary force for adsorption and suitable space for crystallization of PCMs,[35,36] indicating that above three porous materials are suitable for the shape stabilization of PCMs.

Table 1 Surface area and porosity parameters of the three porous materials

Samples	BET surface area (m^2 g^{-1})	Average pore diameter (nm)	Total pore volume (mL g^{-1})
ATP	136	11.2	0.38
A-ATP	174	9.7	0.42
Si-ATP	136	13.6	0.46

3.3 Shape-stabilized ability of the supporting materials

The shape-stabilized ability of Si-ATP for paraffin was visually observed *via* three types of FSPCMs that were prepared by

Fig. 5 Nitrogen adsorption−desorption and pore size distribution curves of the three porous materials: (a) nitrogen adsorption−desorption isotherms, and (b) pore size distributions.

Fig. 6 Comparison of shape-stabilized ability of the three porous materials for paraffin ($m_{\text{porous material}} : m_{\text{paraffin}} = 5 : 3$, 1.0 g supporting material and 0.6 g paraffin for each case).

manually mixed at 80 °C, and the optical images of the three composites were shown in Fig. 6. It can be seen that Si-ATP/paraffin-3 shows no liquid leakage and agglomeration as compared to ATP/paraffin-1 and A-ATP/paraffin-2, indicating that the shape-stabilized ability of Si-ATP for paraffin was enhanced, which resulted from Si-ATP tightly intertwined with the paraffin under the capillary action and intermolecular interaction owing to the honeycomb porous structures of Si-ATP and their *n*-alkyl chains compatibility.

The crystallinity of paraffin in the composites was analyzed by XRD tests, the results as shown in Fig. 7. Although the crystallization peaks of paraffin in the composites were shifted slightly compared with pure paraffin, which may be due to the paraffin molecules contacted with the pore walls of supporting materials changed their crystallization behavior,[35] several typical characteristic crystalline peaks derived from paraffin at 21.3°, 23.7° and ATP at 8.4°, 19.8°, 26.6° are still observed in Fig. 7(a),[15,37] indicating that the crystalline property of paraffin was not significantly affected by the porous structures of the three supporting materials and only physical interpenetration in the pore canals were applied. However, the XRD peaks of paraffin in Si-ATP/paraffin were stronger than those in ATP/paraffin and A-ATP/paraffin are shown in Fig. 7(b), demonstrating that the Si-ATP supported more paraffin due to its great lipophilic property could provide a stronger capacity of adsorbing organic substances. Meanwhile, the morphologies of FSPCMs were observed by SEM analysis, corresponding results as shown in Fig. 4(g, h and i), and as expected, ATP and A-ATP had a certain degree of aggregation in the composites on account of their inferior compatibility with paraffin, but Si-ATP well dispersed in the composite and showed a better compatibility with paraffin, which could further confine the flow of paraffin during the phase change process and enhance its shape-stabilized ability for organic PCMs.

3.4 Thermal analysis of the FSPCMs

The phase change temperature and latent heat are two important parameters characterizing the thermal energy storage capacity of the FSPCMs, which can be obtained from the DSC measurements. The DSC curves of the FSPCMs and pure

paraffin are illustrated in Fig. 8, and the melting temperature (T_m) and crystallization temperature (T_c), melting enthalpy (ΔH_m) and crystallization enthalpy (ΔH_m) were obtained from the DSC curves and summarized in Table 2. Because the supporting materials had no contribution to the latent heat of the composites, thus, the latent heat of the FSPCMs was mainly determined by the amount of paraffin in the supporting materials. The mass fraction of paraffin in the composites can be calculated by the following equation:[38]

$$\text{paraffin content} = \frac{\Delta H_{m,com} + \Delta H_{c,com}}{\Delta H_m + \Delta H_c} \quad (1)$$

where $\Delta H_{m,com}$ and $\Delta H_{c,com}$ are the melting enthalpy and crystallization enthalpy of the composite PCMs, respectively; ΔH_m and ΔH_c are the melting enthalpy and crystallization enthalpy of the pure paraffin, respectively.

As shown in Fig. 8(a) and Table 2, there existed a big difference in the thermal energy storage densities among these FSPCMs prepared by solution absorption method. The mass fraction of crystallized paraffin in Si-ATP/paraffin was far greater than that of ATP/paraffin and A-ATP/paraffin, indicating that Si-ATP has a higher absorption capacity to firmly grasp more paraffin in ethanol solution, resulting in increasing of thermal energy storage density in the composite. By contrast, some paraffin molecules adsorbed on the surface of ATP and A-ATP falling off quickly in this dynamic preparation process for lacking good compatibility between each other. The contents of paraffin in the ATP/paraffin, A-ATP/paraffin and Si-ATP/paraffin yielded a latent heat of fusion for 13.7 J g^{-1}, 26.9 J g^{-1} and 69.6 J g^{-1}, respectively.

Vacuum impregnation is a commonly used method for porous materials to prepare FSPCMs, the porous materials based composites which were prepared *via* the vacuum impregnation usually had a higher thermal energy storage densities than those prepared by natural immersion, especially for the porous materials with fine pores.[39] These FSPCMs obtained by vacuum impregnation and solution absorption methods were compared to further confirm the supporting capacity of Si-ATP for paraffin, the results as shown in Fig. 8(b, c) and Table 2. It can be seen that the melting enthalpies of V-ATP/paraffin and V-A-ATP/paraffin increased dramatically
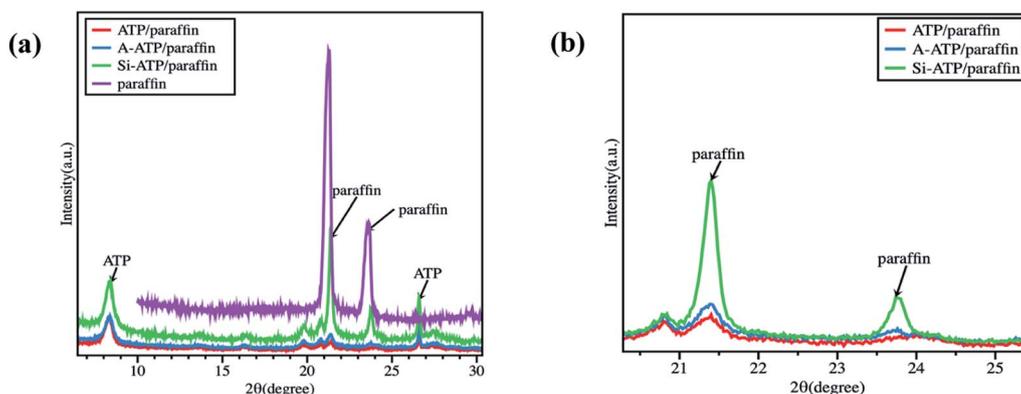

Fig. 7 (a) XRD diagrams of the pure paraffin and FSPCMs; (b) Comparison of paraffin crystallization peaks in FSPCMs (2θ rang from 20–25°).
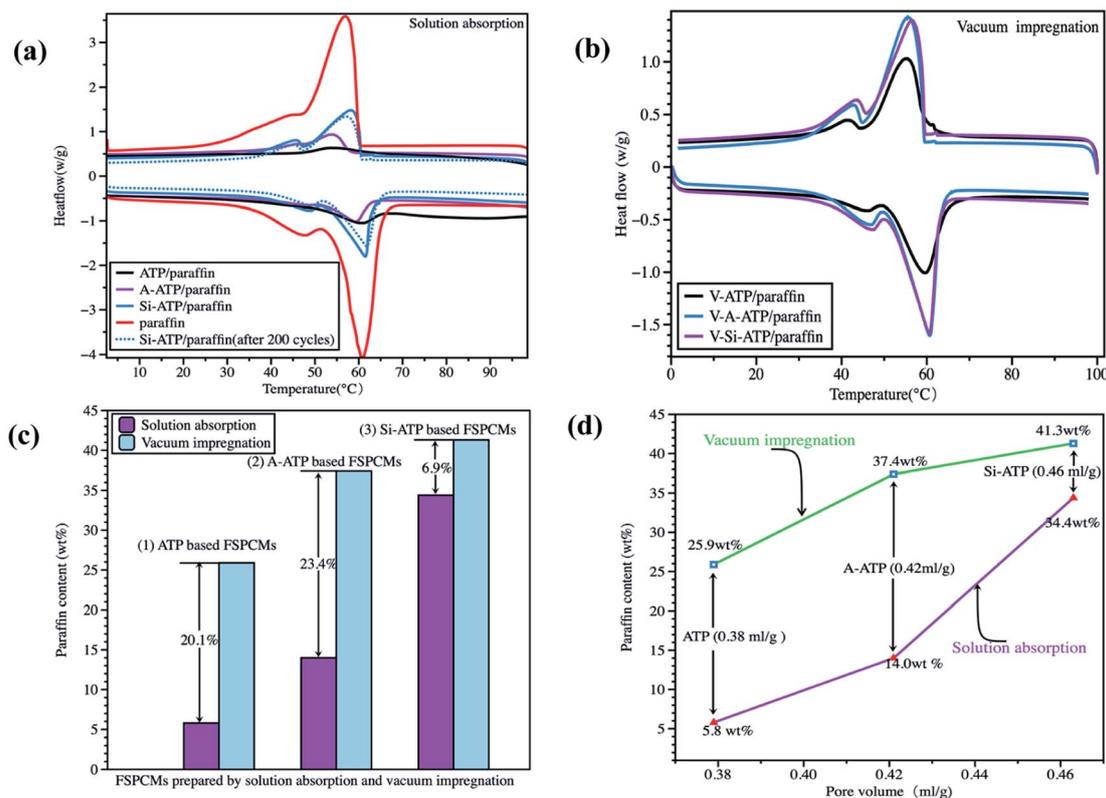
Fig. 8 (a) DSC curves of the FSPCMs prepared by solution absorption; (b) DSC curves of the FSPCMs prepared by vacuum impregnation; (c) a comparison of the FSPCMs prepared by solution absorption and vacuum impregnation; (d) paraffin content in the FSPCMs supported by porous materials with different pore volumes.

Table 2 DSC data of these ATP-supported FSPCMs

Samples	Preparation methods		Melting process		Cooling process		Paraffin content (wt%)
			T_m (°C)	ΔH_m (J g^{-1})	T_c (°C)	ΔH_c (J g^{-1})	
Paraffin	—		60.5	202.1	56.9	202.8	100
ATP/paraffin	Solution absorption		60.3	13.7	53.8	9.7	5.8
A-ATP/paraffin	Solution absorption		59.2	26.9	53.9	29.8	14.0
Si-ATP/paraffin	Solution absorption	1 cycle	61.5	69.6	58.1	69.7	34.4
		100 cycles	61.5	71.2	57.7	71.7	35.3
		200 cycles	61.8	71.2	57.2	68.4	34.5
V-ATP/paraffin	Vacuum impregnation		59.6	50.9	55.2	54.0	25.9
V-A-ATP/paraffin	Vacuum impregnation		60.6	74.9	56.7	76.7	37.4
V–Si-ATP/paraffin	Vacuum impregnation		60.7	83.7	55.5	83.5	41.3

compared with the ATP/paraffin and A-ATP/paraffin, their paraffin content increased by 20.1 wt% and 23.4 wt% resulted in corresponding melting enthalpies increased by 271.5% and 178.4%, respectively, demonstrating that a large portion of the voids in ATP and A-ATP were not well filled with paraffin when paraffin was supported *via* the solution absorption method. However, the paraffin content in V-Si-ATP/paraffin had no significant changes as compared to Si-ATP/paraffin, indicating that most of the pore canals in Si-ATP were well filled with paraffin when paraffin was supported *via* both preparation methods. The above results indicated that the supporting

capacity of Si-ATP for paraffin was significantly enhanced, which resulted from its stronger adsorbing capacity for organic substances and improving compatibility with paraffin. It is worth mentioning that V-Si-ATP/paraffin had a thermal energy storage density of 83.7 J g^{-1}, which was 64.4% higher than 50.9 J g^{-1} of the V-ATP/paraffin.

The effect of pore volumes of supporting materials on the shape-stabilization of PCMs was also analyzed, and the results as shown in Fig. 8(d), it can be seen that regardless of preparation method, the thermal energy storage densities of these resulting FSPCMs were gradually increased with an increase in
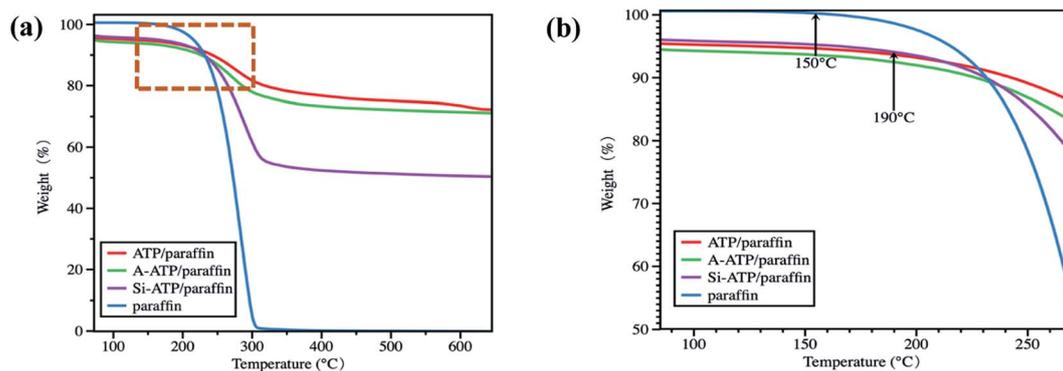
Fig. 9 (a) TGA curves of the pure paraffin and FSPCMs; (b) a part of curves from temperature range of 100–250 °C.

Table 3 Comparison of some porous materials based FSPCMs from literature and this study

Composite PCMs	T_m (°C)	ΔH_m (J g^{-1})	T_c (°C)	ΔH_c(J g^{-1})	Main methods	Ref.
CA/MA(20wt)-vermiculite	19.8	27.5	17.1	31.4	Vacuum impregnation	20
LA/CNTs(5–10 nm)	37.8	54.6	—	—	Vacuum impregnation	21
CA/PA- attapulgite	21.8	48.2	—	—	Vacuum impregnation	25
Paraffin/palygorskite	—	59.3	—	58.4	Vacuum impregnation	27
SA/S-ATP	53.6	73.2	52.8	76.6	Solution polymerization, vacuum impregnation	28
Paraffin RT21/EPO	16.3	60.9	24.6	61.8	Direct impregnation, vacuum impregnation	40
Paraffin/diatomite	36.6	53.2	40.0	58.8	Direct impregnation	41
Paraffin/expended vermiculite (EVM-800)	27.0	77.6	25.1	71.5	Calcined and vacuum impregnation method	42
Paraffin/bentonite	41.7	39.8	43.4	39.0	Solution intercalation	43
RT20/montmorillonite	20.8	53.6	—	—	Direct impregnation	44
Si-ATP/paraffin	52.4	69.6	60.5	69.7	Solution absorption	This work
V–Si-ATP/paraffin	50.4	83.7	59.4	83.5	Vacuum impregnation	This work

the pore volumes of the three porous materials. It's expected that, within limits, the porous materials with more pore volumes are conducive to supporting more PCMs, which in turn will enhance the thermal energy storage densities of the resulting FSPCMs.

3.5 Thermal stability and durability of the FSPCMs

Thermal stability and durability of the Si-ATP/paraffin were evaluated by thermo-gravimetric analysis and thermal cycling test. TGA curves of the pure paraffin and FSPCMs were displayed in Fig. 9.

Fig. 9(a) exhibits that the mass degradation temperature of paraffin range from 150–300 °C and degraded roughly at around 200 °C, which showed a worst thermal stability among the samples. As for these ATP-supported FSPCMs, the weight loss stage occurred between 190–350 °C, which was related to the degradation of alkyl chains as well as a small mass of zeolite water and crystal water in ATP. In addition, the weight loss speed of paraffin in the composites was slower than that of pristine paraffin due to the confinement effect of pore networks on the free movement of paraffin molecules.[19,28] It can be seen from Fig. 9(b) that the initial mass decomposition temperatures of these composites are higher than the pure paraffin, indicating that ATP-supported FSPCMs have a better thermal stability than pure paraffin, and the Si-ATP/paraffin can meet

the thermal stability requirements of most practical applications. Furthermore, as shown in Fig. 8(a) and Table 2, Si-ATP/paraffin still had a high latent heat after suffering 200 melting and freezing cycles, and its thermal energy storage capacity and phase transition temperature changed very little as compared to first cycle, indicating that Si-ATP/paraffin has good thermal durability.

In comparison to some porous materials based FSPCMs from literature and this study, as shown in Table 3, the thermal energy storage densities of the FSPCMs supported by Si-ATP were superior to most porous materials based composites, showing a good thermal energy storage ability, and the Si-ATP/paraffin exhibits great potential applications in thermal energy storage and management.

4. Conclusions

A facile one-step organic modification method of ATP with cost-effective and environmental-friendly characteristics was developed. The chlorosilane-modified ATP (Si-ATP) shows a honeycomb porous structures with increased pore volumes and possesses great hydrophobic and lipophilic properties, which are beneficial to capturing and confining more organic PCMs, thereby eliminating the leakage threat of the liquid and increasing the thermal energy storage densities of the resulting composites. A series of FSPCMs were designed by using three

types of ATP as the supporting materials and paraffin as the latent heat storage units. The results showed that the shape-stabilized ability of Si-ATP for paraffin was significantly enhanced due to a stronger capacity of adsorbing organic substances caused by its great lipophilic property, and the thermal energy storage densities of the resulting FSPCMs were gradually increased with an increase in the pore volumes of the three supporting materials. The Si-ATP based FSPCM yielded an optimal latent heat of 83.7 J g^{-1}, which was 64.4% higher than the pristine ATP based composite. The Si-ATP/paraffin has good thermal stability and durability, its thermal energy storage capacity and phase transition temperature were nearly unchanged after 200 repeated thermal cycles, exhibiting great potential applications in thermal energy storage and management.

Conflicts of interest

There are no conflicts to declare.

Acknowledgements

References

1 Y. Q. Li, Y. A. Samad, K. Polychronopoulou, S. M. Alhassan and K. Liao, From biomass to high performance solar-thermal and electric-thermal energy conversion and storage materials, *J. Mater. Chem. A*, 2014, **2**, 7759–7765.

2 I. Gur, K. Sawyer and R. Prasher, Searching for a better thermal battery, *Science*, 2012, **6075**, 1454–1455.

3 S. Raoux, W. Welnic and D. Ielmini, Phase change materials and their application to nonvolatile memories, *Chem. Rev.*, 2010, **1**, 240–267.

4 A. Kasaeian, L. bahrami, F. Pourfayaz, E. Khodabandeh and W. M. Yan, Experimental studies on the applications of PCMs and nano-PCMs in buildings: a critical review, *Energy Build.*, 2017, **154**, 96–112.

5 D. Lencer, M. Salinga and M. Wuttig, Design rules for phase-change materials in data storage applications, *Adv. Mater.*, 2011, **18**, 2030–2058.

6 B. Zalba, J. M. Marin, L. F. Cabeza and H. Mehling, Review on thermal energy storage with phase change: materials, heat transfer analysis and applications, *Appl. Therm. Eng.*, 2003, **23**, 251–283.

7 J. Li, J. Huang and M. Cao, Properties enhancement of phase-change materials *via* silica and Al honeycomb panels for the thermal management of LiFeO$_4$ batteries, *Appl. Therm. Eng*, 2018, **131**, 660–668.

8 K. O. Lee, M. A. Medina, X. Sun and X. Jin, Thermal performance of phase change materials (PCM)-enhanced cellulose insulation in passive solar residential building walls, *Sol. Energy*, 2018, **163**, 113–121.

9 M. Khosrojerdi and S. M. Mortazavi, Impregnation of a porous material with a PCM on a cotton fabric and the effect of vacuum on thermo-regulating textiles, *J. Therm. Anal. Calorim.*, 2013, **114**, 1111–1119.

10 J. Jing, H. Wu, Y. Shao, X. Qi, J. Yang and Y. Wang, Melamine foam-supported form-stable phase change materials with simultaneous thermal energy storage and shape memory properties for thermal management of electronic devices, *ACS Appl. Mater. Interfaces*, 2019, **11**, 19252–19259.

11 M. M. A. Khan, R. Saidur and F. A. Al-Sulaiman, A review for phase change materials (PCMs) in solar absorption refrigeration systems, *Renewable Sustainable Energy Rev.*, 2017, **76**, 105–137.

12 T. X. Li, S. Wu, T. Yan, J. X. Xu and R. Z. Wang, A novel solid-gas thermochemical multilevel sorption thermal battery for cascaded solar thermal energy storage, *Appl. Energy*, 2016, **161**, 1–10.

13 C. Vélez, M. Khayet and J. M. Ortiz de Zárate, Temperature-dependent thermal properties of solid/liquid phase change even-numbered n-alkanes: n-Hexadecane, n-octadecane and n-eicosane, *Appl. Energy*, 2015, **143**, 383–394.

14 W. Kong, X. Fu, Z. Liu, C. Zhou and J. Lei, A facile synthesis of solid-solid phase change material for thermal energy storage, *Appl. Therm. Eng.*, 2017, **117**, 622–628.

15 D. Wu, B. Ni, Y. Liu, S. Chen and H. Zhang, Preparation and characterization of side-chain liquid crystal polymer/paraffin composites as form-stable phase change materials, *J. Mater. Chem.*, 2015, **3**, 9645–9657.

16 D. G. Prajapati and B. Kandasubramanian, Biodegradable polymeric solid framework-based organic phase change materials for thermal energy storage, *Ind. Eng. Chem. Res.*, 2019, **58**, 10652–10677.

17 M. M. Umair, Y. Zhang, K. Iqbal, S. F. Zhang and B. T. Tang, Novel strategies and supporting materials applied to shape-stabilize organic phase change materials for thermal energy storage-A review, *Appl. Energy*, 2019, **235**, 846–873.

18 Q. S. Lian, Y. Li, A. A. S. Sayyed, J. Cheng and J. Y. Zhang, Facile Strategy in Designing Epoxy/Paraffin Multiple Phase Change Materials for Thermal Energy Storage Applications, *ACS Sustainable Chem. Eng.*, 2018, **6**, 3375–3384.

19 Y. F. Cao, D. L. Fan, S. H. Lin, L. Y. Mu, F. T. T. Ng and Q. M. Pan, Phase change materials based on comb-like polynorbornenes and octadecylamine-functionalized graphene oxide nanosheets for thermal energy storage, *Chem. Eng. J.*, 2020, **389**, 124318.

20 A. Karaipekli and A. Sari, Capric-myristic acid/vermiculite composite as form-stable phase change material for thermal energy storage, *Sol. Energy*, 2009, **83**, 323–332.

21 Y. H. Feng, R. Z. Wei, Z. Huang, X. X. Zhang and G. Wang, Thermal properties of lauric acid filled in carbon nanotubes as shape-stabilized phase change materials, *Phys. Chem. Chem. Phys.*, 2018, **20**, 7772–7780.

22 H. M. Yang, A. D. Tang, J. Ouyang, M. Li and S. Mann, From natural attapulgite to mesoporous materials: methodology, characterization and structural evolution, *J. Phys. Chem. B*, 2010, **114**, 2390–2398.

23 W. L. Haden and I. A. Schwint, Attapulgite:its properties and applications, *Ind. Eng. Chem.*, 1967, **59**, 58–69.

24 Y. H. Ma, W. M. Fang and X. J. Ma, The research and application progress of attapulgite, *Mater. Rev.*, 2006, **20**, 43–46.

25 M. Li, Z. Wu and H. Kao, Study on preparation, structure and thermal energy storage property of capric-palmitic acid/attapulgite composite phase change materials, *Appl. Energy*, 2011, **88**, 3125–3132.

26 S. Song, L. Dong, S. Chen, H. Xie and C. Xiong, Stearic-capric acid eutectic/activated attapulgite composie as form-stable phase change material for thermal energy storage, *Energy Convers. Manag.*, 2014, **81**, 306–311.

27 T. Shi, S. S. Li, H. Zhang and Z. Li, Preparation of Palygorskite-based phase change composites for thermal energy storage and their applications in trombe walls, *J. Wuhan Univ. Technol.*, 2017, **32**, 1306–1317.

28 W. D. Liang, P. S. Chen, H. X. Sun, Z. Q. Zhu and A. Li, Innovative spongy attapulgite loaded with n-carboxylic acids as composite phase change materials for thermal energy storage, *RSC Adv.*, 2014, **4**, 38535–38541.

29 J. Li, L. Yan, H. Y. Li, J. P. Li, F. Zha and Z. Q. Lei, A facile one-step spray-coating process for the fabrication of a superhydrophobic attapulgite coated mesh for use in oil/water separation, *RSC Adv.*, 2015, **5**, 53802–53808.

30 Q. Zhou, Q. Gao, W. J. Luo, C. J. Yan, Z. N. Ji and P. Duan, One-step synthesis of amino-functionalized attapulgite clay nanoparticles adsorbent by hydrothermal carbonization of chitosan for removal of methylene blue from wastewater, *Colloids Surf., A*, 2015, **470**, 248–257.

31 X. Y. Yang, X. B. Wang, J. Yang, J. Li and L. Wan, Functionalization of graphene using trimethoxysilanes and its reinforcement on polypropylene nanocomposites, *Chem. Phys. Lett.*, 2013, **570**, 125–131.

32 J. C. Groen, L. A. A. Peffer and J. Pérez-Ramírez, Pore size determination in modified micro-and mesoporous materials, Pitfalls and limitations in gas adsorption data analysis, *Microporous Mesoporous Mater.*, 2003, **60**, 1–17.

33 K. S. W. Sing, D. H. Everett, R. A. W. Haul, L. Moscou, R. A. Pierotti, J. Rouquerol and T. Siemieniewska, Reporting physisorption data for gas/solid systems with special reference to the determination of surface area and porosity, *Pure Appl. Chem.*, 1985, **57**, 603–619.

34 H. Gao and X. Fang, Research progress of the attapulgite modification method, *Resour. Dev. Mark.*, 2008, **24**, 1090–1093.

35 C. Y. Wang, L. L. Feng, W. Li, J. Zheng, W. H. Tian and X. G. Li, Shape-stabilized phase change materials based on polyethylene glycol/porous carbon composite: The influence of the pore structure of the carbon materials, *Sol. Energy Mater. Sol. Cells*, 2012, **105**, 21–26.

36 X. Py, R. Olives and S. Mauran, Paraffin/porous–graphite–matrix composite as a high and constant power thermal storage material, *Int. J. Heat Mass Transfer*, 2001, **44**, 2727–2737.

37 J. Tang, B. Mu, L. Zong, M. Zheng and A. Wang, Facile and green fabrication of magnetically recyclable carboxyl-functionalized attapulgite/carbon nanocomposites derived from spent bleaching earth for wastewater treatment, *Chem. Eng. J.*, 2017, **322**, 102–114.

38 J. F. Su, L. X. Wang, L. Ren, Z. Huang and X. W. Meng, Preparation and characterization of polyurethane microcapsules containing n-octadecane with styrene-maleic anhydride as a surfactant by interfacial polycondensation, *J. Appl. Polym. Sci.*, 2006, **102**, 4996–5006.

39 M. Xin, M. Fang, Z. Huang, Y. Liu, Y. Huang, R. Wen, T. Qian and X. Wu, Enhanced thermal properties of novel shape-stabilized PEG composite phase change materials with radial mesoporous silica sphere for thermal energy storage, *Sci. Rep.*, 2015, **5**, 12964.

40 S. Ramakrishnan, J. Sanjayan, X. Wang, M. Alam and J. Wilson, A novel paraffin/expanded perlite composite phase change material for prevention of PCM leakage in cementitious composites, *Appl. Energy*, 2015, **157**, 85–94.

41 K. Yeliz, E. Orkun and G. Ozgur, Easy and industrially applicable impregnation process for preparation of diatomite-based phase change material nanocomposites for thermal energy storage, *Appl. Therm. Eng.*, 2015, **91**, 759–766.

42 B. W. Xu, H. Y. Ma, Z. Y. Lu and Z. J. Li, Paraffin/expanded vermiculite composite phase change material as aggregate for developing lightweight thermal energy storage cement-based composites, *Appl. Energy*, 2015, **160**, 358–367.

43 M. Li, Z. S. Wu, H. T. Kao and J. M. Tan, Experimental investigation of preparation and thermal performances of paraffin/bentonite composite phase change material, *Energy Convers. Manage.*, 2011, **52**, 3275–3281.

44 X. M. Fang, Z. G. Zhang and Z. H. Chen, Study on preparation of montmorillonite- based composite phase change materials and their applications in thermal storage building materials, *Energy Convers. Manage.*, 2008, **49**, 718–723.